Microtubule Dynamics in Fish Melanophores

Vladimir I. Rodionov,*‡ Soo-Siang Lim,§ Vladimir I. Gelfand,‖ and Gary G. Borisy*

*Laboratory of Molecular Biology, University of Wisconsin, Madison, Wisconsin 53706; ‡A. N. Belozersky Institute of Physico-Chemical Biology, Moscow State University, Moscow 119899, Russia; §Department of Anatomy, Indiana University Medical Center, Indianapolis, Indiana 46202; and ‖Department of Cell and Structural Biology, University of Illinois at Urbana-Champaign, Urbana, Illinois 61801

Abstract. We have studied the dynamics of microtubules in black tetra (*Gymnocorymbus ternetzi*) melanophores to test the possible correlation of microtubule stability and intracellular particle transport. X-rhodamine- or caged fluorescein-conjugated tubulin were microinjected and visualized by fluorescence digital imaging using a cooled charge coupled device and videomicroscopy. Microtubule dynamics were evaluated by determining the time course of tubulin incorporation after pulse injection, by time lapse observation, and by quantitation of fluorescence redistribution after photobleaching and photoactivation. The time course experiments showed that the kinetics of incorporation of labeled tubulin into microtubules were similar for cells with aggregated or dispersed pigment with most microtubules becoming fully labeled within 15–20 min after injection. Quantitation by fluorescence redistribution after photobleaching and photoactivation confirmed that microtubule turnover was rapid in both states, $t_{1/2}$ = 3.5 ± 1.5 and 6.1 ± 3.0 min for cells with aggregated and dispersed pigment, respectively. In addition, immunostaining with antibodies specific to posttranslationally modified α-tubulin, which is usually enriched in stable microtubules, showed that microtubules composed exclusively of detyrosinated tubulin were absent and microtubules containing acetylated tubulin were sparse. We conclude that the microtubules of melanophores are very dynamic, that their dynamic properties do not depend critically on the state of pigment distribution, and that their stabilization is not a prerequisite for intracellular transport.

One of the most prominent features of microtubules is their dynamic behavior, the ability to rapidly exchange subunits between soluble and polymer pools (for review see Gelfand and Bershadsky, 1991). Dynamics of microtubules is under cellular control. One of the most striking examples of modification of microtubule dynamics is its increase during the transition from interphase to mitosis (Saxton et al., 1984; Belmont et al., 1990). In interphase cells, microtubule dynamics may vary from one cell type to another and, in some cases, depend on the degree of cell differentiation. For example, muscle fiber differentiation is accompanied by microtubule stabilization (Gundersen et al., 1984) and differentiation of retina also involves stabilization of a special class of microtubules (Arregni and Barra, 1989; Sale et al., 1988). Even in a single cell, it is often possible to reveal subpopulations of microtubules that differ from each other in dynamic properties. Such subpopulations were found in cells of different types, in epithelial cells (Pepperkok et al., 1990; Wadsworth and McGrail, 1990), monocytes (Cassimeris et al., 1986), and fibroblasts (Webster et al., 1987; Schulze and Kirschner, 1987). Stable microtubules are usually enriched in posttranslationally modified (detyrosinated and acetylated) α-tubulin (Kreis, 1987; Schulze et al., 1987; Webster and Borisy, 1989), which can be revealed by immunocytochemical staining with specific antibodies.

The molecular mechanisms and functional significance of differential stability of interphase microtubules are not yet understood. It appears that there is some correlation between microtubule stability and their involvement in intracellular transport phenomena. For example, bundles of stable noncentrosomal microtubules that traverse differentiated MDCK cells (Baccalao et al., 1989) are presumably involved in intracellular transport because biosynthetic and transcytotic pathways of protein traffic to the apical surface are dramatically altered by the microtubule-disrupting drug nocodazole (Brietfield et al., 1990). In neurons, microtubules that support axonal transport down to a nerve terminal and back to the cell body are enriched in stable domains (Baas and Black, 1990).

The fish melanophore provides a most dramatic example of a cell highly specialized in intracellular particle transport. These cells contain thousands of pigment granules, melanosomes, which in response to neurohumoral stimuli, either move to the cell center to form a dense spherical aggregate or redisperse throughout the cytoplasm (reviewed in Schliwa,

Address correspondence to Vladimir I. Rodionov, Laboratory of Molecular Biology, University of Wisconsin, Madison, WI. Phone: (608) 262-4581; fax: (608) 262-4570.

1984; Obika, 1986). These pigment motions are clearly microtubule dependent because disruption of microtubules blocks pigment dispersion and prevents directed pigment aggregation (Schliwa and Bereiter-Hahn, 1973; Murphy and Tilney, 1974; Beckerle and Porter, 1983). In addition, melanosome aggregation may be mediated by the retrograde microtubule-dependent motor protein dynein (Beckerle and Porter, 1982; Ogawa et al., 1987; Haimo and Fenton, 1989. *J. Cell Biol.* 107:245*a*), and dispersion is supported by the anterograde motor protein kinesin (Rodionov et al., 1991). Thus, pigment motion in fish melanophores is microtubule dependent, and we have chosen these cells to study the possible relationship between microtubule dynamics and intracellular transport.

To evaluate microtubule dynamics in melanophores, we used injections of tubulin tagged with X-rhodamine or with caged fluorescein. We then followed the time course of incorporation of X-rhodamine–tubulin into microtubule networks or measured kinetics of fluorescence redistribution after photobleaching of X-rhodamine–labeled tubulin or photoactivation of caged fluorescein–labeled tubulin. Our data demonstrate that microtubules form a dynamic array in melanophores and that stabilization of microtubules is not a necessary condition of their involvement in intracellular transport.

Materials and Methods

Melanophore Cultures

Melanophores were dissociated from the *G. ternetzi* fish scales by collagenase treatment as described in detail previously (Gyoeva et al., 1987). Cells were washed three to five times in Ringer solution and placed onto coverslips mounted with silicone vacuum grease (Dow Corning Corp., Midland, MI) in 35-mm tissue culture dishes with 18-mm holes. Coverslips with photoetched locator grids (Bellco Biotechnology, Bellco Glass Inc., Vineland, NJ) that were covered with carbon or poly-D-lysine were used to enhance melanophore spreading. Cells were allowed to spread for 30 min in a drop of Ringer solution at 30°C and covered with Dulbecco's modified Eagle's medium buffered with 20 mM Hepes and supplemented with 15% fetal calf serum, 100 IU/ml penicillin, 0.12 mg/ml streptomycin, and 0.1 mg/ml gentamycin. Melanophores were cultured in the same medium overnight at 30°C. Pigment aggregation was induced by 10^{-5} M adrenalin. For pigment dispersion, cells were transferred into Ringer solution with 5 mM caffeine.

Preparation and Microinjection of Derivatized Tubulin

Labeling of porcine brain tubulin with X-rhodamine was performed as described previously (Sammak and Borisy, 1988). Samples used for microinjections were at a protein concentration of ~4–6 mg/ml and a dye/protein molar ratio of 0.5:1.0. Caged fluorescein–tubulin was prepared essentially as described by Mitchison (1989). The samples of this derivative used for microinjection were at a concentration of 15–20 mg/ml and a dye/protein ratio of 0.2:0.3. All samples of tagged tubulin were distributed into 5–10-μl aliquots immediately after synthesis and purification and stored in liquid nitrogen. Just before use, an aliquot was thawed and spun at 20,000 *g* for 30 min to remove particulates.

Microinjections were performed according to the method of Graessmann and Graessmann (1976) with micropipettes with a tip diameter of ~1 μm using a microinjector (Narishige USA, Inc., Greenvale, NY) or a gas-tight syringe (Hamilton Co., Reno, NV) as a pressure source. Melanophores with dispersed pigment were injected at the cell centers, and melanophores with aggregated pigment were injected at the base of the spherical melanosome mass. After injection, cells were incubated at room temperature to allow incorporation of labeled tubulin into microtubules.

Photobleaching and Photoactivation

The apparatus used for photobleaching and photoactivation has been described in detail previously (Gorbsky et al., 1987; Lim et al., 1989). Briefly, the beam of a 3-W argon ion laser (Spectra-Physics Anal., Fremont, CA) was channeled into the epi-illumination system of a microscope (IM-35; Carl Zeiss, Inc., Thornwood, NY). A 100x, 1.3 aperture objective was used, and a cylindrical lens was positioned to produce a focused 4 × 57-μm beam cross-section in the specimen plane. For the photobleaching experiments, the laser was operated at 514 nm and 200 mW for 200 ms, and the beam was attenuated by a 0.6-OD neutral density filter. Irradiation at this laser intensity did not disrupt microtubules (see Results). Photoactivation was performed using 334-, 351-, and 364-nm bands of the laser at 100 mW for 100 ms. The images of a bleached zone and of a fluorescent bar were obtained at different time intervals after photobleaching and photoactivation and were used for subsequent quantitative analysis.

Image Acquisition and Analysis

A Zeiss IM-35 microscope equipped with a 100-W mercury arc lamp was used for fluorescence microscopy of both living and fixed melanophores. The light passed through ultraviolet and infrared blocking filters, neutral density filters, and either rhodamine wide-band filter (in the case of experiments with living X-rhodamine–injected cells) or through the rhodamine/fluorescein selective filter set. A silicon-intensified target video camera (Dage-MTI, Inc., Michigan City, IN) was used for focusing, but images for data analysis were acquired with a charge-coupled device (CCD)[1] camera (series 200; Photometrics Ltd., Tuscon, AZ) containing a 384 × 576-pixel chip (Thompson CSF TH7882CDA) that was thermoelectrically cooled to −50°C to reduce the dark current noise. Images were digitized to 14-bit depth and stored on a write once read many drive optical disk (model 3363; IBM Corp., Armonk, NY). A video processor (Image-1; Universal Imaging Corp., West Chester, PA) was used for image processing and quantitation of photobleaching experiments. Negatives for the photographs were obtained from the digital files using a film recorder.

Quantitation of the photoactivation data was performed using Photometrics CCD 200 software. The images of fluorescent bars were first improved by flat fielding to make a correction for uneven illumination. Images were then displayed on the video monitor, and a rectangle was delineated using a mouse that surrounded the image of a bar. Fluorescence intensity values of the pixels within the rectangle were integrated and computed. A rectangle of exactly the same dimensions was positioned outside of the bar image, fluorescence intensity of the background was quantitated, and the value for a background was subtracted from the value for the bar. The data for each cell were expressed as a percent of fluorescence intensity remaining with increasing time after photoactivation. The 100% value was taken as the fluorescence intensity of a bar immediately after photoactivation. Data for cells with dispersed and aggregated pigment were plotted and analyzed using SigmaPlot (Jandel Scientific Corp., San Rafael, CA).

Immunofluorescence Staining of Melanophore Microtubules

For immunostaining, cells were rinsed three times with PBS, lysed with 0.5% Triton X-100 in PHEM (60 mM Pipes, 25 mM Hepes, 10 mM EGTA, and 2 mM MgCl, pH 6.8), supplemented with 10 μM taxol for 3 min, and fixed with 0.5% glutaraldehyde in PBS for 20 min. Cells were then rinsed three times with PBS, and glutaraldehyde was quenched with two changes of 2 mg/ml sodium borohydride in PBS. Cells were then washed three times with PBS and incubated with a primary and then with a secondary antibody for 30 min at 37°C. In the case of double immunostaining, melanophores were incubated sequentially with each of the primary antibodies and then with each of the secondary antibodies. All antibody solutions were prepared in PBS containing 2 mg/ml bovine serum albumin. After each incubation, cells were washed for 15 min with three changes of PBS.

Primary antibodies used were mouse monoclonal anti-β-tubulin (Amersham Corp., Arlington Heights, IL), rat YL1/2 anti-Tyr tubulin (Kilmartin et al., 1982) (Accurate Chemical & Scientific Corp., Westbury, NY), rabbit anti-Glu-tubulin (Gundersen et al., 1984) (a gift from Dr. J. Chloe Bulinski, Columbia University, New York), and mouse 6-11B-1 anti-acetylated tubulin (Piperno and Fuller, 1985) (a gift from Dr. Gianni Piperno, Rockefeller University, New York). Secondary antibodies were fluorescein-conjugated anti-mouse IgG, rhodamine-conjugated anti-rat IgG, and fluorescein-conjugated anti-rabbit IgG (Jackson ImmunoResearch, West Grove, PA).

Chemical acetylation in vitro was performed as described by Piperno et

1. *Abbreviation used in this paper*: CCD, charge-coupled device.

al. (1987). Briefly, cells were fixed with methanol at −70°C for 6 min, incubated in 0.1% acetic anhydride in 1 M sodium phosphate pH 8 for 1 min, and rehydrated in PBS. Melanophores were then immunostained with 6-11B-1 antibody.

Results

Five experimental approaches were used to evaluate microtubule dynamics in melanophores: (*a*) the kinetics of incorporation after pulse injection of X-rhodamine–labeled tubulin was compared qualitatively for cells with aggregated and dispersed pigment; (*b*) steady-state analysis of microtubule polymerization and depolymerization was performed by time lapse observation of X-rhodamine–labeled microtubules; (*c*) melanophores were immunostained with antibodies to post-translationally modified (detyrosinated or acetylated) tubulin known to be enriched for stable microtubules; (*d*) the rate of microtubule turnover was quantitated by analysis of recovery of fluorescence after photobleaching in melanophores injected with X-rhodamine–tubulin; and (*e*) the rate of microtubule turnover was also quantitated by analysis of dissipation of fluorescence after photoactivation in melanophores injected with caged fluorescein–tubulin.

Kinetics of Incorporation of X-Rhodamine Tubulin into Microtubules after Pulse Injection

Melanophores microinjected with tagged tubulin remained fully viable after injections and responded normally to adrenalin and caffeine treatments by showing pigment aggregation and redispersion. Fig. 1, shows a cell injected with X-rhodamine–tubulin and incubated at room temperature for 2 h after injection. Fig. 1, *a* and *c* are the phase contrast images, and Fig. 1, *b* and *d* are the images of the microtubule network obtained with a CCD camera. Microtubules fully incorporated labeled tubulin by 2 h of incubation (Fig. 1, *b* and *d*), and the cell aggregated pigment with normal velocity (Fig. 1 *c*).

To follow the kinetics of incorporation of fluorescently labeled tubulin into microtubules, cells with dispersed or aggregated pigment were injected with X-rhodamine–tubulin, lysed at different time intervals after injection, fixed, and stained with tubulin antibody and with a secondary antibody labeled with fluorescein. The CCD images of microtubules incorporating X-rhodamine–labeled tubulin were compared with the images of all microtubules stained with tubulin antibody.

Low magnification images of melanophores fixed within 1–2 min after injection showed that as in other cells (Soltys and Borisy, 1985; Schulze and Kirschner, 1986), fluorescently labeled subunits initially incorporated into the short fragments of microtubules that corresponded to their distal ends. In melanophores with dispersed pigment, short microtubules connected to the cell center were also seen (data not shown).

We analyzed in more detail the kinetics of incorporation of labeled tubulin subunits into microtubules located at the cell periphery because most of them could be traced individually. Since microtubules are very numerous in melanophores (Schliwa and Euteneuer, 1978) and they are especially abundant around the cell center, we followed the incorporation of labeled subunits into microtubules located at the cell periphery that could be traced individually. Fig. 2 illustrates the kinetics of incorporation of labeled tubulin into microtubules of melanophores with dispersed or aggregated pigment. At 3 min after injection, X-rhodamine–tagged tubulin was found to incorporate predominantly into distal ends of preexisting microtubules (Fig. 2, *upper left*). With increasing time after injection, there was an increase in the number of microtubules that became labeled all along their length, and after 20–30 min, most of the microtubules seemed to be labeled (Fig. 2, *middle left*), but complete labeling was observed only ~60 min after injection (Fig. 2, *lower left*).

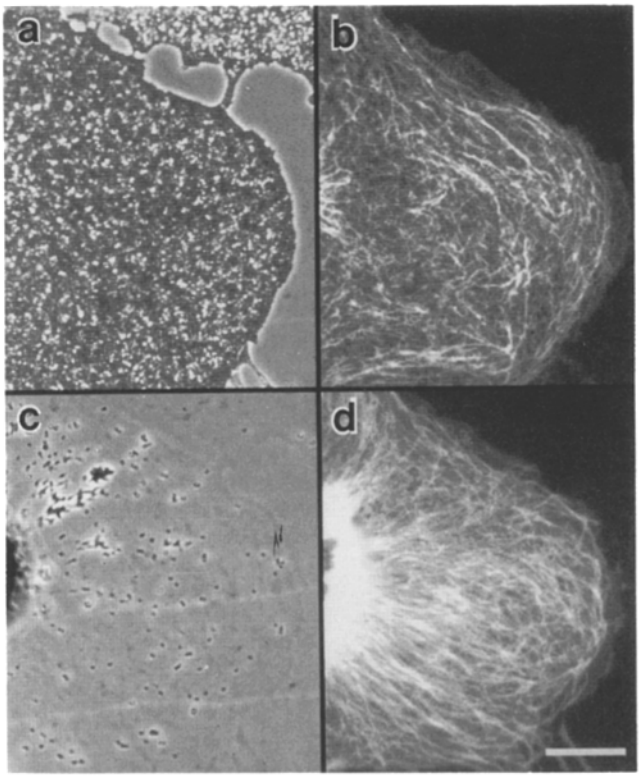

Figure 1. Melanophores microinjected with X-rhodamine–labeled tubulin retain the ability to aggregate pigment in response to adrenalin. Melanophore with dispersed pigment was injected with X-rhodamine–tubulin and incubated for 2 h at 30°C. Adrenalin was then added to a final concentration of 10^{-5} M. Phase contrast images (*a* and *c*) show pigment distribution and CCD fluorescence images (*b* and *d*) show microtubule distribution before (*a* and *b*) and after (*c* and *d*) adrenalin treatment. Bar, 10 μm.

The kinetics of labeling of microtubules in the cells with aggregated pigment did not differ significantly from that in the cells with dispersed pigment (Fig. 2, *right column*). Again, after 3 min, only some of the microtubules became labeled, and many of these showed incorporation at their ends (Fig. 2, *upper right*). After 20–30 min, the majority of the microtubules incorporated rhodamine-tagged tubulin (Fig. 2, *middle right*), although complete labeling was achieved only 1 h after injection (Fig. 2, *lower right*).

Thus, the incorporation experiments showed that melanophore microtubules were capable of rapid turnover and that the turnover rates of microtubules in the cells with aggregated and dispersed pigment did not differ significantly.

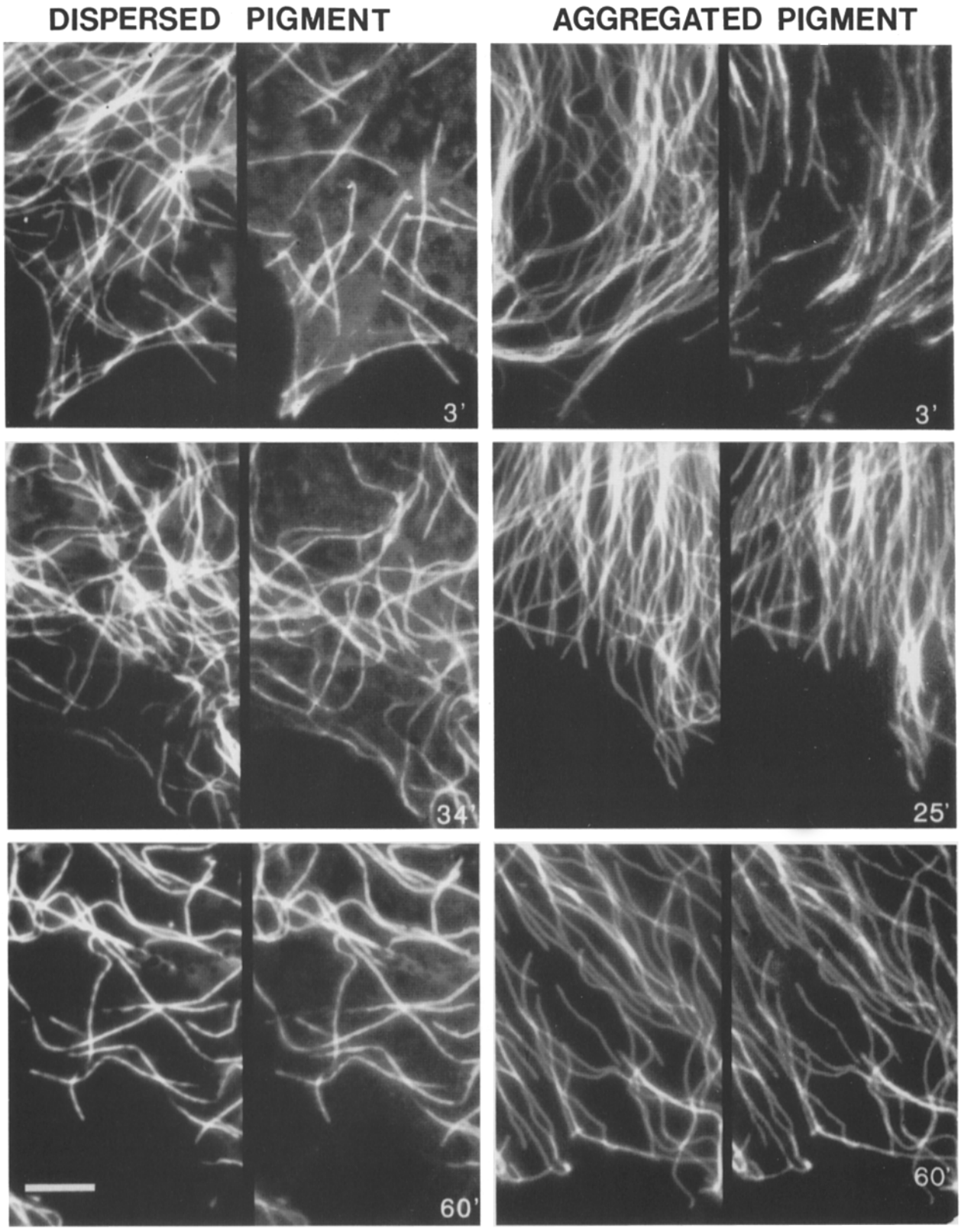

Figure 2. Kinetics of incorporation of X-rhodamine–labeled tubulin into microtubules in melanophores. Cells with dispersed (*left column*) or aggregated (*right column*) pigment were injected with X-rhodamine–tubulin, incubated for the various time intervals, fixed, and stained with tubulin antibodies and with secondary fluorescein-labeled antibodies. Numbers indicate time in minutes after injection. At each time point, the left image of a pair shows all microtubules revealed by antitubulin staining, and right image displays microtubules that incorporated labeled tubulin. Bar, 5 μm.

Steady-state Analysis of Polymerization and Depolymerization of Microtubules in Melanophores

To confirm the dynamic nature of individual microtubules, we tried to observe microtubule behavior in the living cell. Melanophores with aggregated or dispersed pigment were injected with X-rhodamine–tubulin and left for 60–80 min at room temperature to equilibrate labeled tubulin with the endogenous pool. As shown in the previous experiments, this time was sufficient to completely label all cellular microtubules. A series of sequential fluorescent images of peripheral parts of the cells was taken at 12-s intervals. Fig. 3 shows an example of a melanophore with aggregated pigment where the individual microtubules could be clearly seen. The ends of four microtubules in the process can be followed on the micrographs. Two of these microtubules (1 and 4) shortened significantly within 36 s, one (microtubule 3) elongated, while the last one (microtubule 2) remained stationary. The same observations were also made on microtubules of melanophores with dispersed pigment (data not shown). Thus, microtubules in both aggregated and dispersed cells were indeed capable of rapid polymerization and depolymerization.

Immunostaining with Antibodies Specific to Posttranslationally Modified Tubulin

Stable microtubules in many cell types are characterized by the presence of posttranslationally modified α-tubulin (Kreis, 1987; Schulze et al., 1987; Webster and Borisy, 1989). One of these modifications is selective removal of the COOH-terminal tyrosine, leaving glutamic acid as a carboxy-terminal residue (for review see Barra et al., 1988), and another is acetylation of the ε-amino group of lysine 40 residue (L'Hernault and Rosenbaum, 1983). Although the functional significance of these modifications is not yet understood, it is clear that in many cases these modifications are good markers of stable microtubules. We thus tested the content of stabilized microtubules in melanophores by immunostaining with the antibodies specific to detyrosinated or acetylated forms of α-tubulin.

Fig. 4, *a* and *b* shows double immunostaining of melanophore microtubules with antibodies specific to tyrosinated and detyrosinated tubulins. Antibodies to tyrosinated tubulin revealed a dense meshwork of uniformly stained microtubules, while microtubules stained with antibodies to detyrosinated tubulin were less numerous, and the staining along their lengths was nonuniform. Superimposition of these images showed that most of the microtubules were composed of tyrosinated tubulin only, while the remaining microtubules were copolymers of modified and unmodified tubulins (not shown). Microtubules that did not contain tyrosinated tubulin were not found.

The 6-11B-1 antibody, which specifically recognized acetylated α-tubulin, stained very short sparse microtubules emanating from the cell center. Such microtubules were clearly seen in the cells with dispersed pigment, where the cell center was not occupied with pigment mass (Fig. 4 *c*). To test whether the poor immunoreactivity of the melanophore microtubules resulted from inaccessibility of the epitope for 6-11B-1 antibody, cells were fixed with methanol and incubated with an excess of acetaldehyde. This procedure induces extensive acetylation of all reactive groups of melanophore proteins, including lysine 40 residue of α-tubulin (Piperno et al., 1987). Fig. 4 *d* shows that the chemical acetylation dramatically enhanced the staining of microtubules. Thus, poor staining of melanophore microtubules with

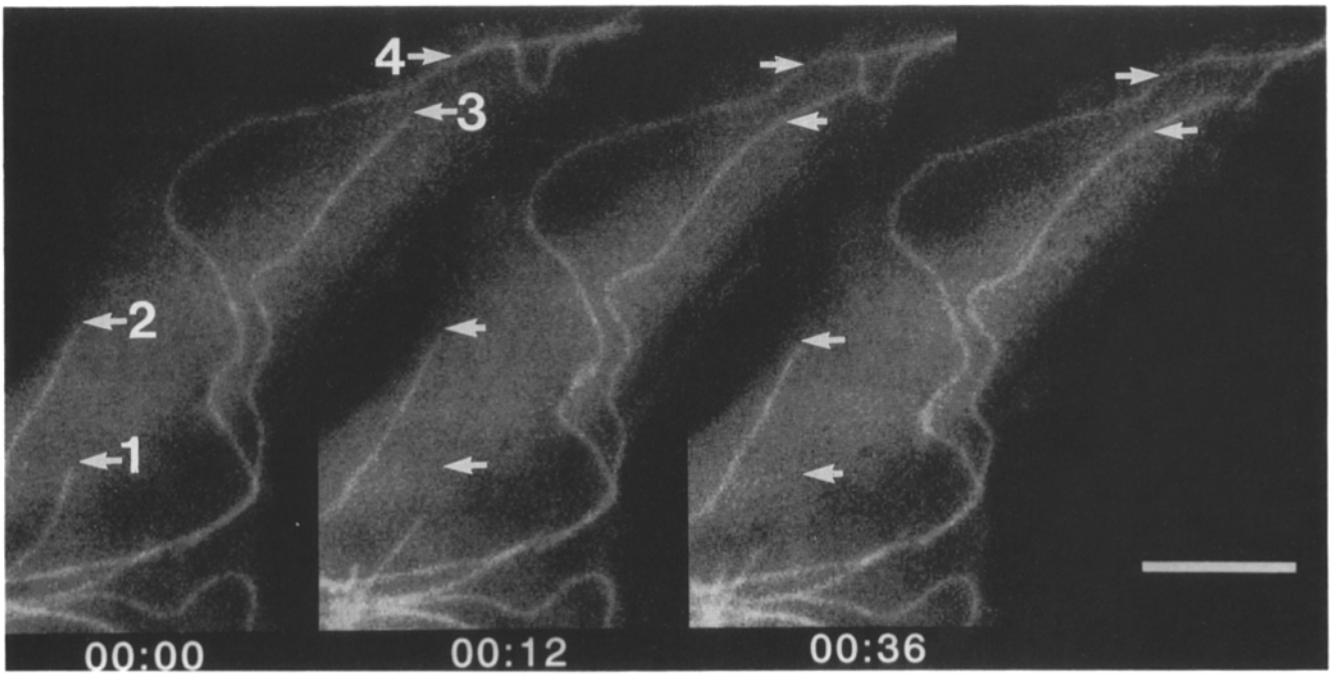

Figure 3. Time lapse analysis of microtubule elongation-shortening in a living melanophore. A cell with aggregated pigment was injected with X-rhodamine–tubulin, and after 2 h of incubation at 30°C, successive microtubule images were obtained at 12-s intervals. Arrows show positions of microtubule ends at the zero time point. During the first 12 s, microtubules 1 and 4 shortened at velocities of 0.15 and 0.13 μm, respectively; microtubules 3 elongated at a velocity of 0.25 μm/s, while microtubule 2 remained stationary. Bar, 5 μm.

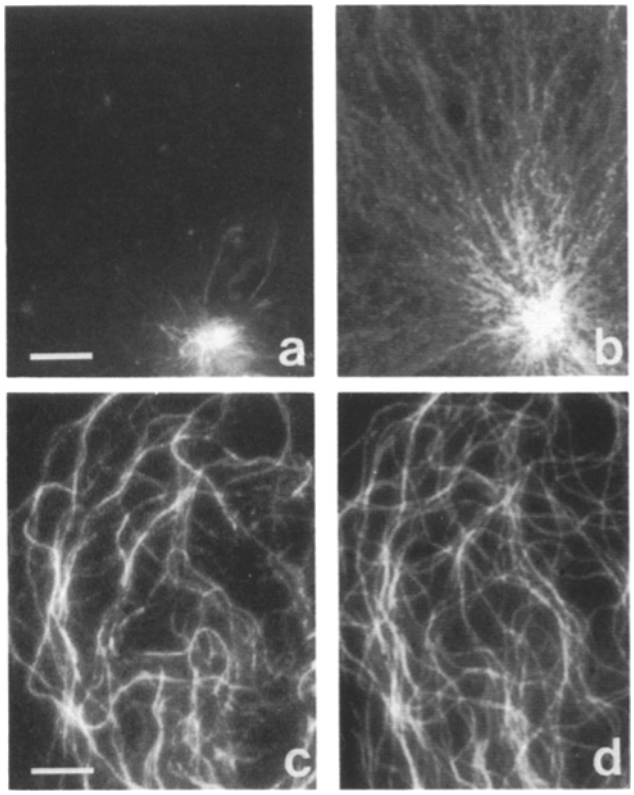

Figure 4. Microtubules enriched in detyrosinated and acetylated α-tubulin in melanophores. Double immunostaining of a melanophore with aggregated pigment with antibodies to detyrosinated (*a*) and tyrosinated (*b*) tubulin. Melanophores with dispersed pigment untreated (*c*) and treated (*d*) with acetaldehyde were stained with the 6-11B-1 antibody specific for acetylated α-tubulin. Bars, 10 μm.

6-11B-1 antibody could not be explained by masking of the Lys 40 of melanophore tubulin.

Thus, the results of immunostaining with antibodies to posttranslationally modified α-tubulin demonstrated that modified (and most probably stable) microtubules are not abundant in melanophores, consistent with the evidence from pulse injection and direct visualization that melanophore microtubules are dynamic.

Quantitation of Microtubule Dynamics Using Photobleaching and Photoactivation

For the quantitative analysis of microtubule dynamics in melanophores, the kinetics of fluorescence redistribution after photobleaching and photoactivation were analyzed.

For the photobleaching experiments, cells were injected with X-rhodamine–tubulin, incubated for 60–120 min for incorporation of labeled tubulin subunits into microtubules, and irradiated with the laser microbeam to produce a bleached zone that was positioned at approximately an equal distance between the cell center and cell margin. The images of the bleached zone were obtained with the CCD camera at increasing time intervals after irradiation and used for quantitative analysis. Immunostaining of irradiated cells with anti-tubulin antibodies showed that under the conditions used for irradiation (see Materials and Methods), the microbeam did not disrupt microtubules (not shown).

Fig. 5 shows a typical example of fluorescence redistribution after photobleaching in a cell with aggregated pigment. To determine the microtubule turnover rate, the profiles of the bleached zone were obtained (Fig. 5 *a*), and the areas under the peaks of reduced fluorescence intensity were measured (data not shown). Analysis of the curve of fluorescence recovery showed that 50% of fluorescence intensity was achieved at ~5 min after photobleaching. As fluorescence recovery in the bleached zone reflects depolymerization and subsequent repolymerization of microtubules, the half time for 50% fluorescence recovery corresponds to the half time of microtubule turnover. High magnification images of the bleached zone indicated that the mechanism of fluorescence recovery was a one-by-one substitution of bleached microtubules by labeled ones in the bleached zone (Fig. 5 *b*). Thus,

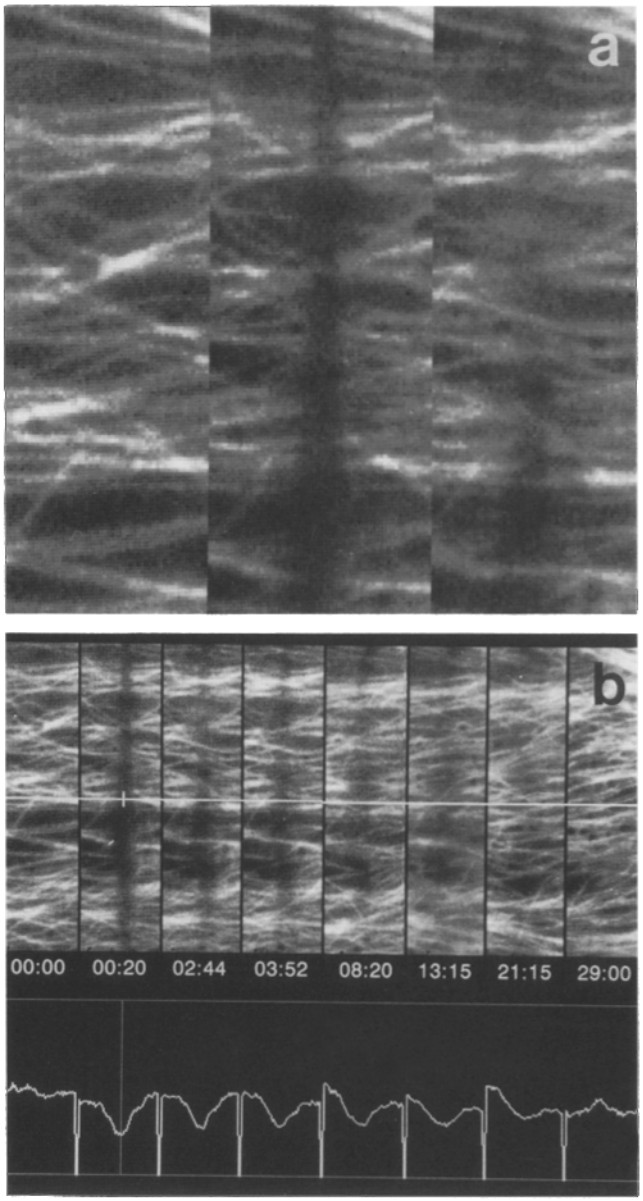

Figure 5. Kinetics of fluorescence recovery after photobleaching in a melanophore with aggregated pigment. (*a*) Lower magnification image and fluorescence intensity profiles in the bleached zone during recovery. (*b*) High magnification image; note one-by-one substitution of bleached for fluorescent microtubules in the bleached zone.

the results of the photobleaching experiments confirmed the rapid turnover of microtubules in melanophores. The photobleaching technique, however, was not readily applicable to cells with dispersed pigment because, if melanosomes were located in the irradiated zone, they absorbed the green energy efficiently, thus inducing irreversible cell damage from heating (not shown; see also Rodionov et al., 1987).

To obtain more precise data on microtubule dynamics in melanophores and to compare directly microtubule turnover rates in cells with aggregated and dispersed pigment, photoactivation experiments were performed. Melanophores with dispersed pigment were injected with caged fluorescein–tubulin and either incubated for 1–4 h or first treated with adrenalin and then incubated for the same period of time for equilibration of labeled tubulin subunits with microtubules. Cells were then irradiated to activate the caged fluorescein. Unlike the irradiation with the green light used in photobleaching experiments, irradiation with long wave UV at comparable power levels did not induce cell damage, and activated zones could be seen both in cells with aggregated and dispersed pigment (not shown). Photoactivation of caged fluorescein did not affect pigment motion and, if the irradiated cells were stimulated with adrenalin or caffeine, melanosomes crossed the fluorescent zone with normal kinetics. The activated zones did not move relative to the cell center, in melanophores with neither aggregated nor with dispersed melanosomes, and they remained detectable for up to 60 min after irradiation.

For the quantitative analysis of fluorescence redistribution, successive images of activated zones were acquired with the CCD camera at different time intervals after photoactivation (Fig. 6), and fluorescence intensities in the activated zones were measured as described in Materials and Methods. Fig. 7 shows the averaged data obtained for cells with dispersed (Fig. 7 *a*) and with aggregated (Fig. 7 *b*) pigment. Fluorescence intensities showed an initial rapid drop (Fig. 7, *a* and *b*, *insets*), followed by a much more slower decrease (Fig. 7, *a* and *b*). The initial drop of fluorescence in the activated zones did not depend on the integrity of cytoplasmic microtubules because it was observed in melanophores treated with nocodazole (10 μM for 5 h) which has been demonstrated to completely disrupt melanophore microtubules (Gyoeva et al., 1987). At the same time, the slow component of fluorescence decay was never observed in nocodazole-treated cells. Therefore, we conclude that the fast drop represents diffusion of soluble tubulin and that the slow decay reflects microtubule turnover.

To determine the half-life time for microtubule turnover, it was necessary to subtract the rapid drop of fluorescence unrelated to the exchange of subunits in microtubules from the total decay of fluorescence in the activated zones. The kinetics of the fast drop of fluorescence was analyzed in more detail in a separate experiment using 10 melanophores injected with caged fluorescein–tubulin and treated with nocodazole. Nocodazole-treated cells were irradiated and the images of fluorescent zones were acquired at 1-s intervals, and the decay data for 10 cells were averaged and approximated by a single exponential curve using the SigmaPlot curve-fitting program. The decay constant for the fast process was calculated to be 0.786^{s-1}, and this value was used as a correction factor in subsequent analysis of the fluorescence decay data for the cells with intact microtubules.

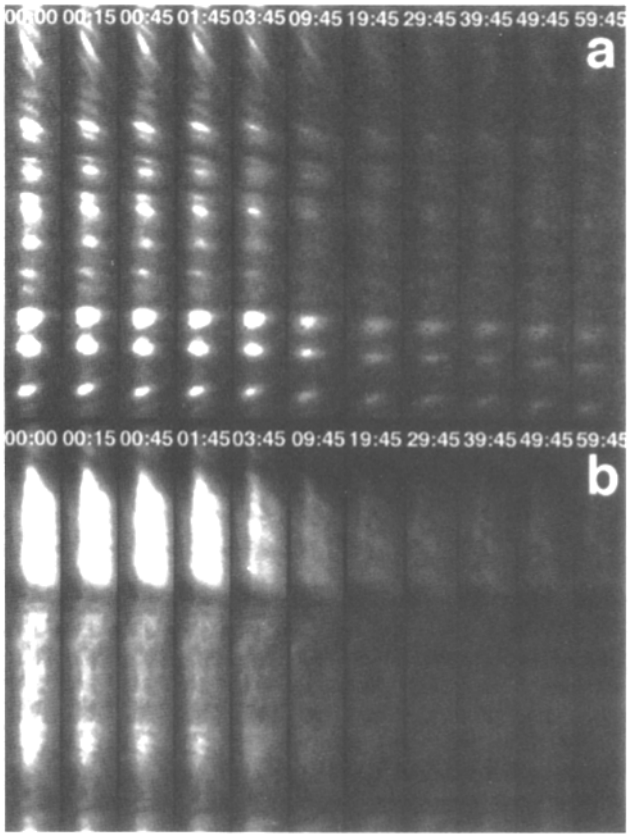

Figure 6. The decay of fluorescence in activated zones in cells with dispersed and aggregated pigment. Fluorescent zones were activated in cells injected with caged fluorescein-tubulin and images of fluorescent zones were obtained with the CCD camera. (*a*) Fluorescent zone in a cell with dispersed pigment. (*b*) Fluorescent zone in a cell with aggregated pigment. Numbers indicate time in minutes: seconds after photoactivation.

To estimate the half times of microtubule turnover in the cells with aggregated and dispersed pigment, fluorescence decay data were approximated by a double exponential curve $y = a \exp(-k\,t) + b \exp(-0.786\,t) + c$. In this equation, $\exp(-k\,t)$ corresponds to the major process that reflects microtubule turnover, and $b \exp(-0.786\,t)$ corresponds to the minor fast drop of fluorescence. The coefficient c measures the amount of the remaining fluorescence, thus indicating the existence of material in the fluorescence zones that failed to exchange with nonfluorescent subunits. The curves that were generated for the cells with dispersed and aggregated pigment fit well to the experimental data (Fig. 7, *a* and *b*). The values for k (the decay constants for the slow process that reflects microtubule turnover) were used for the calculation of the half times of microtubule turnover, which were estimated to be 3.1 ± 1.5 min for cells with aggregated pigment and 6.0 ± 3.0 min for cells with dispersed pigment. Thus, quantitation of microtubule dynamics using photoactivation showed that microtubule dynamics in melanophores was indeed fast in both cells with aggregated and dispersed pigment. Turnover may be somewhat faster in cells with aggregated pigment, but the errors associated with the determined values are too large to permit a strong conclusion on this point.

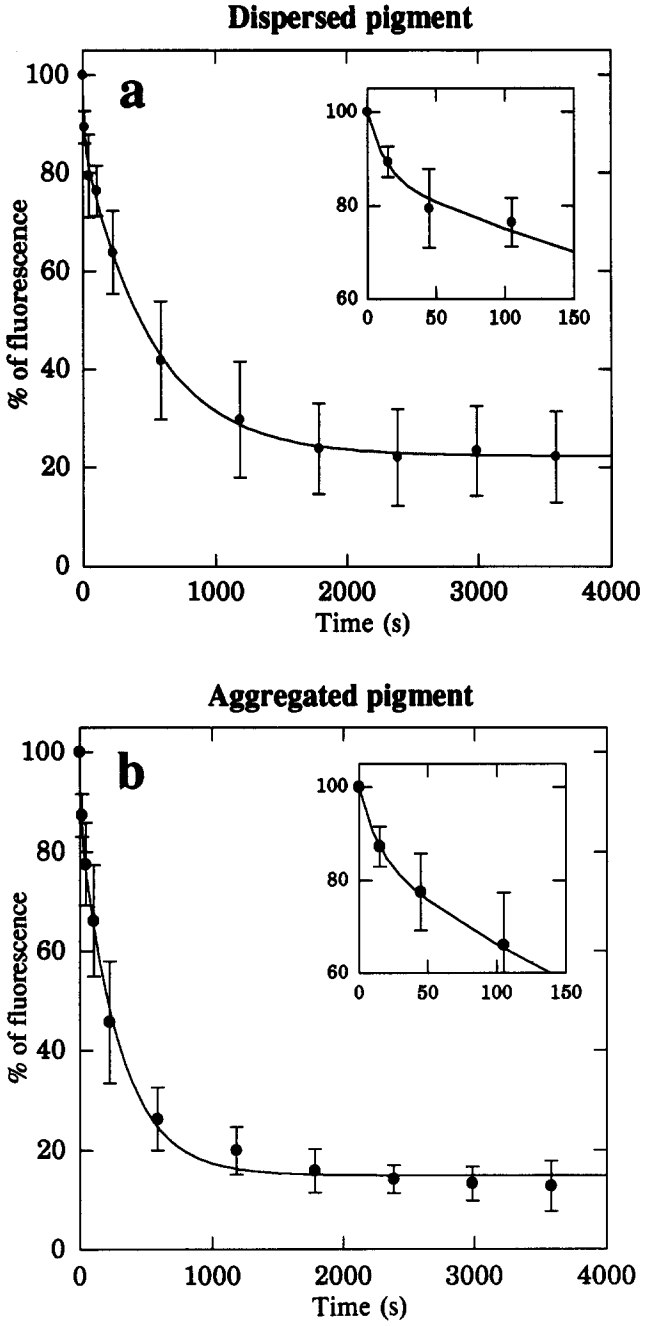

Figure 7. Kinetics of fluorescence decay in photoactivated zones in melanophores with dispersed and aggregated pigment. Melanophores were injected with caged fluorescein-tubulin, incubated for 1–4 h at 30°C, and fluorescent bars were induced by irradiation with UV light. The images of fluorescent bars at different time intervals after irradiation were acquired with a CCD camera and used for quantitation of fluorescence. The fluorescence decay data were expressed for each cell as a percent of fluorescence remaining as a function of time after photoactivation. The data were averaged separately for 12 cells with dispersed pigment and 12 cells with aggregated pigment. The mean values are shown on the graphs by filled circles (the error bars are SEM). Continuous lines demonstrate the approximation of kinetics of fluorescence decay by the double exponential curves (see text for the details). (*a*) Dispersed and (*b*) aggregated pigment. Insets are the same graphs rescaled to show the initial fast drop of fluorescence.

Discussion

Evaluation of Microtubule Dynamics in Melanophores

Though the organization of the microtubule system in chromatophores has been the subject of extensive studies during the last few decades, the data about their dynamic properties appear to be controversial. For example, in some studies colchicine was shown to depolymerize microtubules in melanophores and erythrophores (Beckerle and Porter, 1983; Schliwa and Bereiter-Hahn, 1973), while in others (Obika et al., 1978), melanophore microtubules were found to be resistant to this drug taken at a concentration as high as 5 mM. In an ultrastructural study, Schliwa and Euteneuer (1978) reported that the number of microtubules in aggregated melanophores was 60% less than in dispersed ones and suggested that microtubule polymerization-depolymerization cycles were involved in melanosome movement. In contrast to this observation, Murphy and Tilney (1974) found that microtubule number in *Fundulus* melanophores was the same in cells with aggregated and dispersed pigment.

In the present work, we used a variety of direct approaches to evaluate for the first time microtubule dynamics in pigment cells, and we showed that microtubules in the black tetra melanophores are surprisingly dynamic. They incorporate labeled tubulin subunits quickly after pulse injection, and they can be seen to lengthen and shorten rapidly. Further, they are not enriched in posttranslationally modified tubulin, which usually marks stable microtubules in the cells.

We quantitated microtubule dynamics in melanophores using the approach of fluorescence redistribution, both after photobleaching and photoactivation. The photoactivation approach with caged fluorescein-labeled tubulin showed exceptional signal/noise ratio (Mitchison, 1989) and turned out to have an additional advantage in contrast to the visible light used for photobleaching. Apparently, the pigment granules in melanophores do not absorb long-wave UV light as much as green radiation and, therefore, photoactivation did not induce detectable cell damage.

The analysis of plots of fluorescence decay showed an initial rapid drop. Such an initial rapid drop was also observed in nocodazole-treated cells and, thus, was not related to microtubule turnover. This rapid process (with a $t_{1/2}$ of ~8 s) most probably reflects the diffusion of tubulin dimers. Comparable rates of diffusion were reported for a photoactivatable dextran of mol w 10,000 that has a Stokes' radius slightly smaller than tubulin (Reinsch et al., 1991).

Some 15–20% of fluorescence remained in the activated zones even after 1 h after irradiation and represents a nonexchangeable fraction of tubulin subunits. The simplest explanation is that this residual fluorescence marks a fraction of stable microtubules that exchange subunits at a very slow rate. However, this result is inconsistent with the pulse incorporation data that show microtubules to be fully labeled by 1 h. Possibly the UV irradiation used to activate the caged fluorescein produced some damage expressed as cross-linked and, therefore, nonexchangeable tubulin.

After correction for the fast-diffusing tubulin, analysis of the data that we interpret to correspond to microtubule turnover allowed an estimate of the decay half time for the slower process. Indeed, the slow process was the major contribution

to the fluorescence decay of the activated zones in both melanophores with aggregated and dispersed pigment, and it was never observed in cells with disrupted microtubules. The half times of microtubule turnover for cells with aggregated and dispersed pigment were estimated to be 3.1 ± 1.5 and 6.0 ± 3.0 min, respectively. Thus, melanophore microtubules appear to be as dynamic as microtubules in fibroblasts (Schulze and Kirschner, 1987; Wadsworth and McGrail, 1990) and more dynamic than microtubules in epithelial cells (Pepperkok et al., 1990; Wadsworth and McGrail, 1990).

Although the average half times for microtubule turnover in cells with aggregated or dispersed pigment differed by a factor of 2, the values for microtubule turnover half times for individual cells in different states of pigment distribution overlapped significantly suggesting heterogeneity in the cell population of limitations in the method of measurement. Nevertheless, we may conclude that the turnover of the majority of microtubules in melanophores is fast, and that their dynamic properties are similar in the cells with aggregated or dispersed pigment.

Possible Roles of Microtubule Dynamics in Melanophores

It is well known that microtubules are especially dynamic in cells that either are capable of fast locomotion or can easily change their shape (Gelfand and Bershadsky, 1991). Fish melanophores neither move nor change their shape on a substrate. Therefore, one might have expected that in these cells, microtubules would be highly stable, similar to those in polarized epithelial cells (Pepperkok et al., 1990), the neuron shaft (Lim et al., 1989; Baas and Black, 1990), or the avian erythrocyte marginal band. However, contrary to these expectations, microtubules in melanophores are very dynamic. Their dynamic behavior is qualitatively similar to that in fibroblasts (Wadsworth and McGrail, 1990), although fibroblasts constantly move on the substrate and change their shape.

Fish melanophores are a classical (Bickle et al., 1966) extreme example of a cell highly specialized in intracellular microtubule-dependent transport, and it is worth considering whether microtubule polymerization and depolymerization in these cells may be directly coupled to the translocation of pigment organelles. The coupling of microtubule dynamics to organelle transport is well documented for mitosis and has been suggested to provide the force for anaphase chromosome separation (Koshland et al., 1988; Coue et al., 1991). However, such coupling has never been demonstrated for interphase cells, and melanophores provide an excellent model for the study of the possible involvement of microtubule dynamics in intracellular transport. The possible role of microtubule dynamics in pigment transport needs further characterization.

The alternative view is that particle movement in melanophores is powered by microtubule motors (Beckerle and Porter, 1982; Rodionov et al., 1991). If this is correct, we must conclude that motor molecules can move organelles along dynamic microtubules, as well as along the more stable microtubules found in neurites and epithelial cells. How can dynamic microtubules provide the tracks for pigment granule movement in melanophores if the time of microtubule turnover is comparable to the aggregation time and much less than that of dispersion? One may suggest two possibilities. First, the microtubule system in melanophores is redundant and each granule contacts with more than one microtubule at any moment in time. In the case of depolymerization of one of the microtubules, another may remain intact and a granule may continue to move along the remaining microtubule. Another possibility is that not only microtubules, but also some other cytoplasmic component, is capable of interacting with granules. In this case, microtubule depolymerization may leave granules stationary interacting with this component waiting for a new microtubule growing and coming into contact with them. Possibly, such a component is the vimentin intermediate filaments that are very abundant in these cells (Gyoeva et al., 1987).

The connection between microtubule dynamics and cell organization is most obvious in cells that change their shape. Although melanophores do not normally change their shape during the process of pigment motion, they show a high level of structural organization of their cytoplasm with a radial arrangement of cytoskeletal structures (Schliwa et al., 1978; Gyoeva et al., 1987). This radial organization determines the direction of motion of pigment granules and is maintained by the array of microtubules. Indeed, the radial organization of the cytoplasm is reestablished in melanophore fragments severed from the parent cell, and rearrangement of microtubules has been shown to be a key event in this reestablishment (McNiven et al., 1984; McNiven and Porter, 1986; 1988). Thus, melanophores retain a latent capacity to adjust their shape, and microtubule dynamics may be important for the maintenance of the radial organization in their cytoplasm.

We wish to thank John Peloquin for the preparation of X-rhodamine- and caged fluorescein-tubulin, Tim Mitchison for the gift of caged fluorescein, and Vadim Arshavsky for the help in the use of SigmaPlot. This work was supported by National Institutes of Health grant GM25062 to G. G. Borisy and by the National Science Foundation grant MCB-901667 to V. I. Gelfand.

Received for publication 12 April 1994.

References

Arregni, C., and H. S. Barra. 1989. Tyrosination state of tubulin and the activity of tubulin-tyrosine ligase and tubulin carboxypeptidase in the developing retina of chick. *J. Neurochem.* 52:1708–1713.

Baas, P. W., and M. M. Black. 1990. Individual microtubules in axons consist of domains that differ in both composition and stability. *J. Neurochem.* 52:1708–1723.

Baccalao, R., C. Antony, C. Dotti, E. Karsenti, E. H. K. Stelzer, K. Simons. 1989. The subcellular organization of Madin-Darby canine kidney cells during formation of a polarized epithelium. *J. Cell Biol.* 109:2817–2832.

Barra, H. S., C. A. Arce, and C. E. Argarana. 1988. Posttranslational tyrosination/detyrosination of tubulin. *Mol. Neurobiol.* 2:133–153.

Beckerle, M. S., and K. R. Porter. 1982. Inhibitors of dynein activity block intracellular transport in erythrophores. *Nature (Lond.).* 295:701–703.

Beckerle, M. C., and K. R. Porter. 1983. Analysis of the role of microtubules and actin in erythrophore intracellular motility. *J. Cell Biol.* 96:354–362.

Belmont, L. D., A. A. Hyman, K. E. Sawin, and T. J. Mitchison. 1990. Real-time visualization of cell cycle-dependent changes in microtubule dynamics in cytoplasmic extracts. *Cell.* 62:579–589.

Bickle, D., L. G. Tilney, and K. R. Porter. 1966. Microtubules and pigment migration in the melanophores of *Fundulus heteroclitus*. *Protoplasma.* 61:322–345.

Brietfield, P. P., W. C. McKinnon, and K. E. Mostow. 1990. Effect of nocodazole on vesicular traffic to the apical and basolateral surfaces of polarized MDCK cells. *J. Cell Biol.* 111:2365–2373.

Cassimeris, L. U., P. Wadsworth, and E. D. Salmon. 1986. Dynamics microtubule depolymerization in monocytes. *J. Cell Biol.* 104:9–18.

Coue, M., V. A. Lombillo, and J. R. McIntosh. 1991. Microtubule depolymer-

ization promotes particle and chromosome movement in vitro. *J. Cell Biol.* 112:1165–1175.
Gelfand, V. I., and A. D. Bershadsky. 1991. Microtubule dynamics: mechanism, regulation, and function. *Annu. Rev. Cell Biol.* 7:93–116.
Gorbsky, G. J., P. J. Sammak, and G. G. Borisy. 1987. Chromosomes move poleward in anaphase along stationary microtubules that coordinately disassemble from their kinetochore ends. *J. Cell Biol.* 104:9–18.
Graessmann, M., and A. Graessmann. 1976. Early simian virus-40 RNA contains information for tumor antigen formation and chromatin replication. *Proc. Natl. Acad. Sci. USA.* 73:366–370.
Gundersen, G. G., M. H. Kalnoski, and J. C. Bulinski. 1984. Distinct populations of microtubules: tyrosinated and nontyrosinated alpha tubulin are distributed differentially in vivo. *Cell.* 38:779–789.
Gyoeva, F. K., E. V. Leonova, V. I. Rodionov, and V. I. Gelfand. 1987. Intermediate filaments in fish melanophores. *J. Cell Sci.* 88:649–655.
Kilmartin, J. V., B. Wright, and C. Milstein. 1982. Rat monoclonal antitubulin antibodies derived by using a new nonsecreting rat cell line. *J. Cell Biol.* 93:576–582.
Koshland, D. E., T. J. Mitchison, and M. W. Kirschner. 1988. Poleward chromosome movement driven by microtubule depolymerization in vitro. *Nature (Lond.).* 331:449–504.
Kreis, T. E. 1987. Microtubules containing detyrosinated tubulin are less dynamic. *EMBO (Eur. Mol. Biol. Organ.) J.* 6:1007–1019.
L'Hernault, S. W., and J. L. Rosenbaum. 1983. Chlamydomonas α-tubulin is post-translationally modified by acetylation on the ϵ-amino-group of a lysin. *Biochemistry.* 24:473–478.
Lim, S.-S., P. J. Sammak, and G. G. Borisy. 1989. Progressive and spatially differentiated stability of microtubules in developing neuronal cells. *J. Cell Biol.* 109:253–263.
McNiven, M. A., M. Wang, and K. R. Porter. 1984. Microtubule polarity and direction of pigment transport reverse simultaneously in surgically severed melanophore arms. *Cell.* 37:753–765.
McNiven, M. A., and K. R. Porter. 1986. Microtubule polarity confers direction to pigment transport in chromatophores. *J. Cell Biol.* 103:1547–1555.
McNiven, M. A., and K. R. Porter. 1988. Organization of microtubules in centrosome-free cytoplasm. *J. Cell Biol.* 106:1593–1605.
Mitchison, T. J. 1989. Poleward microtubule flux in the mitotic spindle: evidence from photoactivation of fluorescence. *J. Cell Biol.* 109:637–652.
Murphy, D. B., and L. G. Tilney. 1974. The role of microtubules in the movement of pigment granules in teleost melanophores. *J. Cell Biol.* 61:757–779.
Obika, M., 1986. Intracellular transport of pigment granules in fish melanophores. *Zool. Sci. (Tokyo).* 3:1–11.
Obika, M., W. A. Turner, Jr., S. Negishi, D. G. Mentez, T. T. Tchen, and J. D. Taylor. 1978. The effects of lumicolchicine and vinblastine on pigment migration in fish chromatophores. *J. Exp. Zool.* 205:95–110.
Ogawa, K., H. Hosoya, E. Yokota, T. Kobayashi, Y. Wakamatsu, and K. Ozato. 1987. Melanoma dynein: evidence that dynein is a general "motor" for microtubule-associated cell motilities. *Eur. J. Cell Biol.* 43:3–9.
Piperno, G., and M. T. Fuller. 1985. Monoclonal antibodies specific for an acetylated form of alpha-tubulin recognize the antigen in cilia and flagella from a variety of organisms. *J. Cell Biol.* 101:2085–2094.
Piperno, G., M. LeDizet, and X.-j. Chang. 1987. Microtubules containing acetylated α-tubulin in mammalian cells in culture. *J. Cell Biol.* 104: 289–302.
Pepperkok, R., M. H. Bre, J. Davoust, and T. Kreis. 1990. Microtubules are stabilized in confluent epithelial cells but not in fibroblasts. *J. Cell Biol.* 1990:3003–3012.
Reinsch, S. S., T. J. Mitchison, and M. Kirschner. 1991. Microtubule polymer assembly and transport during axonal elongation. *J. Cell Biol.* 115:365–379.
Rodionov, V. I., F. K. Gyoeva, and V. I. Gelfand. 1991. Kinesin is responsible for centrifugal movement of pigment granules in melanophores. *Proc. Natl. Acad. Sci. USA.* 88:4956–4960.
Rodionov, V. I., A. Vardanyan, V. F. Kamalov, and V. I. Gelfand. 1987. Movement of melanosomes in melanophore fragments, obtained by laser microbeam irradiation. *Cell Biol. Int. Rep.* 11:566–575.
Sale, W. S., J. C. Besharse, and G. Piperno. 1988. Distribution of acetylated alpha-tubulin in retina and in vitro-assembled microtubules. *Cell Motil. Cytoskeleton.* 9:243–253.
Sammak, P. J., and G. G. Borisy. 1988. Detection of single fluorescent microtubules and methods for determining their dynamics in living cells. *Cell Motil. Cytoskeleton.* 10:238–245.
Saxton, W. M., D. L. Stemple, R. J. Leslie, E. D. Salmon, M. Zavortink, and J. R. McIntosh. 1984. Tubulin dynamics in cultured mammalian cells. *J. Cell Biol.* 99:2175–2186.
Schliwa, M., and J. Bereiter-Hahn. 1973. Pigment movements in fish melanophores: morphological and physiological studies. III. The effects of colchicine, and vinblastine. *Z. Zellforsch.* 147:127–148.
Schliwa, M. 1978. Microtubule apparatus of melanophores. Three-dimensional organization. *J. Cell Biol.* 76:605–614.
Schliwa, M., M. Osborn, and K. Weber. 1978. Microtubule system of isolated fish melanophores as revealed by immunofluorescence microscopy. *J. Cell Biol.* 76:229–236.
Schliwa, M. 1984. Mechanisms of intracellular organelle transport. *Cell Muscle Motil.* 5:1–82.
Schulze, E., and M. Kirschner. 1986. Microtubule dynamics in interphase cells. *J. Cell Biol.* 102:1020–1031.
Schulze, E., D. J. Asai, J. C. Bulinski, and M. Kirschner. 1987. Posttranslational modification and microtubule stability. *J. Cell Biol.* 105:2167–2177.
Schulze, E., and M. Kirschner. 1987. Dynamic and stable populations of microtubules in cells. *J. Cell Biol.* 104:277–288.
Soltys, B. J., and G. G. Borisy. 1985. Polymerization of tubulin in vivo: direct evidence for assembly onto microtubule ends and from centrosomes. *J. Cell Biol.* 100:1682–1689.
Wadsworth, P., and M. McGrail. 1990. Interphase microtubule dynamics are cell specific. *J. Cell Sci.* 95:23–32.
Webster, D. R., and G. G. Borisy. 1989. Microtubules are acetylated in domains that turn over slowly. *J. Cell Sci.* 92:57–65.
Webster, D. R., G. G. Gunderson, J. C. Bulinski, and G. G. Borisy. 1987. Differential turnover of tyrosinated and detyrosinated microtubules. *Proc. Natl. Acad. Sci. USA.* 84:9040–9044.